Available online at www.sciencedirect.com
ScienceDirect
International Journal of Solids and Structures 44 (2007) 6450–6472
INTERNATIONAL JOURNAL OF SOLIDS AND STRUCTURES
www.elsevier.com/locate/ijsolstr

Exact solutions of functionally graded piezoelectric shells under cylindrical bending

Chih-Ping Wu *, Yun-Siang Syu

Department of Civil Engineering, National Cheng Kung University, Taiwan, ROC

Received 7 November 2006; received in revised form 23 February 2007
Available online 2 March 2007

Abstract

Within a framework of the three-dimensional (3D) piezoelectricity, we present asymptotic formulations of functionally graded (FG) piezoelectric cylindrical shells under cylindrical bending type of electromechanical loads using the method of perturbation. Without loss of generality, the material properties are regarded to be heterogeneous through the thickness coordinate. Afterwards, they are further specified to be constants in single-layer homogeneous shells and to obey an identical exponent-law in FG shells. The transverse normal load and normal electric displacement (or electric potential) are, respectively, applied on the lateral surfaces of the shells. The cylindrical shells are considered to be fully simple supports at the edges in the circumferential direction and with a large value of length in the axial direction. The present asymptotic formulations are applied to several benchmark problems. The coupled electro-elastic effect on the structural behavior of FG piezoelectric shells is evaluated. The influence of the material property gradient index on the variables of electric and mechanical fields is studied.

Keywords: FG material; Piezoelectricity; Shells; Cylindrical bending; Exact solutions; Static analysis

1. Introduction

Since numerous articles have reported that laminated piezoelectric structures often produce interfacial stress concentration and large value of residual thermal stresses at the interfaces between elastic and piezoelectric layers as they are subjected to a variety of electro-thermo-mechanical loads (Heyliger, 1997; Kapuria et al., 1997; Chen et al., 1999; Wang and Zhong, 2003). That fact due to a sudden change of material properties occurring at the interfaces between two dissimilar materials may limit the lifetime of this conventional type of intelligent or smart structures.

In recent years, a new class of functionally graded (FG) piezoelectric materials has been widely used as intelligent or smart structures in the engineering applications. Unlike a sudden change of material properties

* Corresponding author. Fax: +886 6 2370804.
E-mail address: cpwu@mail.ncku.edu.tw (C.-P. Wu).

0020-7683/$ - see front matter © 2007 Elsevier Ltd. All rights reserved.
doi:10.1016/j.ijsolstr.2007.02.037

in laminated piezoelectric structures, the material properties of FG structures are gradually changed and dependent upon the composition of the constituent materials. Since the interfacial stresses in the FG piezoelectric plates and shells change smoothly, the aforementioned drawbacks in laminated piezoelectric structures are reduced.

Recently, several researchers have worked on determination of exact solutions of FG piezoelectric plates and shells due to the increasing usage of FG materials. Ramirez et al. (2006a) presented an approximately three-dimensional (3D) solution for the coupled static analysis of FG piezoelectric plates using a discrete layer approach. Two types of FG materials have been considered in their analysis where the through-the-thickness distributions of material properties are taken as the power-law and quadratic functions. Based on the state space approach, Zhong and Shang (2003, 2005) presented an exact 3D analysis for a FG piezoelectric plate under electro-thermo-mechanical loads. The material properties have been assumed to obey the same exponent-law dependence on the thickness coordinate. The influence of the power of the assumed exponent function on the structural behavior has been examined. Based on the Stroh-like formalism, Lu et al. (2006) studied the similar static problem of FG piezoelectric plates. The appropriate range of thin plate theories has been discussed on a basis of their 3D solutions. Several exact 3D solutions for a variety of coupled electro-mechanical problems have also been presented. The free vibration problems of laminated circular piezoelectric plates and discs and laminated magneto-electro-elastic plates have been studied by Heyliger and Ramirez (2000) and Ramirez et al. (2006b). Based on the pseudo-Stroh formalism, Pan (2001) presented exact solutions for the static analysis of linearly magneto-electro-elastic, simply supported, multilayered rectangular plates. The pseudo-Stroh formalism has also been applied for the exact analysis of FG and layered magneto-electro-elastic plates by Pan and Han (2005).

The cylindrical bending problems of orthotropic and laminated piezoelectric structures have been used as the benchmark problems to assess a newly proposed 3D or 2D analysis (Ray et al., 1992; Heyliger and Brooks, 1996; Dumir et al., 1997; Chen et al., 1996). It has been concluded that the assumption for the linear variations of deformations and electric potential across the thickness coordinate may lead to the satisfactory results for the structural behavior as the ratio of length-to-thickness is larger than six (Ray et al., 1992).

After a close literature survey, we have realized that there are two approaches, the transfer matrix method (or so-called the propagator matrix method) and power series method, commonly used for the exact analysis of single-layer homogeneous, multilayered and FG elastic and piezoelectric structures. An alternative analytical approach, the asymptotic approach, has been proposed for the previous subjects by Wu and his colleagues (1996, 2002, 2005, 2005, 2006). The 3D asymptotic formulations for the static, dynamic, buckling and nonlinear analyses of laminated elastic or piezoelectric shells have been developed. It has been shown that the asymptotic solutions are accurate and the rate of convergence is rapid in comparison with the accurate results available in the literature.

Since the asymptotic approach may account for an arbitrary function of material property through the thickness, we extend its application to exact cylindrical bending analysis of FG piezoelectric shells. Based on the generalized Hamilton's principle, Tiersten (1969) indicated that there are two possibilities for electric loading conditions on the lateral surfaces (i.e., either normal electric displacement or electric potential is prescribed). Hence, we aim at developing two different asymptotic formulations corresponding to the cases of prescribed normal electric displacement and electric potential, respectively. Afterwards, these two asymptotic formulations are applied for several benchmark problems of single-layer homogeneous and FG piezoelectric shells.

2. Basic equations of 3D piezoelectricity

A FG orthotropic piezoelectric cylindrical shell with a large value of length is considered and shown in Fig. 1. The cylindrical coordinates system with variables x, θ, r is used and located on the middle surface of the shell. $2h$ and R stand for the total thickness and the curvature radii to the middle surface of the shell, respectively. The radial coordinate r is also represented as $r = R + \zeta$ where ζ is the thickness coordinate measured from the middle surface of the shell.

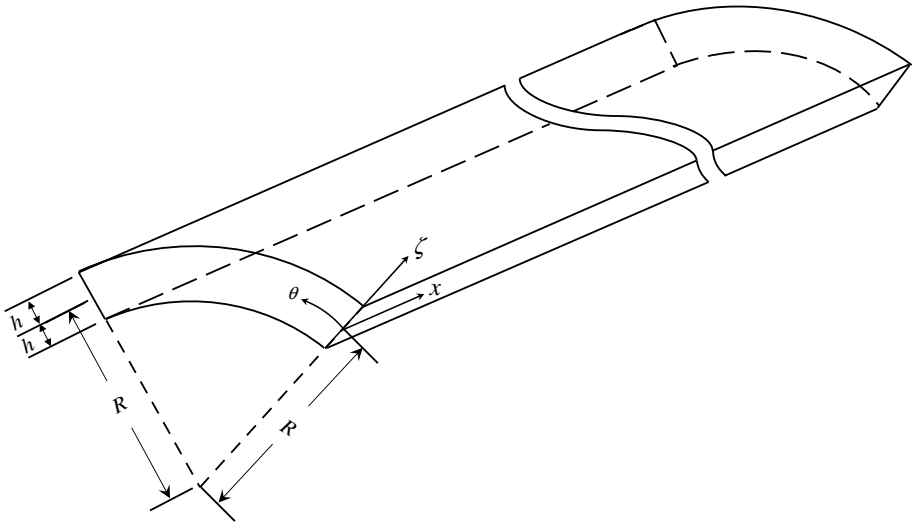

Fig. 1. The dimension and coordinate system for a cylindrical shell with a very long length.

The constitutive equations valid for the nature of symmetry class of piezoelectric material are given by

$$\sigma_i = c_{ij}\varepsilon_j - e_{ki}E_k, \tag{1}$$

$$D_k = e_{kj}\varepsilon_j + \eta_{kl}E_l, \tag{2}$$

where σ_i, ε_j denote the contracted notation for the stress and strain components, respectively. D_k and E_k denote the components of electric displacement and electric fields, respectively. The indices i and j range from 1 to 6, and k and l range from 1 to 3. c_{ij}, e_{ij} and η_{ij} are the elastic, piezoelectric and dielectric coefficients, respectively, relative to the geometrical axes of the cylindrical shell. The material properties are considered as heterogeneous through the thickness (i.e., $c_{ij}(\zeta)$, $e_{ij}(\zeta)$ and $\eta_{ij}(\zeta)$).

In the cases of cylindrical bending problems, all the field variables must be the functions of circumferential and thickness coordinates only, not the axial coordinate. Hence, all the relative derivatives of the field variables with respect to the axial coordinate will be identical to zero in the present formulation.

The strain–displacement relations are given by

$$\begin{Bmatrix} \varepsilon_x \\ \varepsilon_\theta \\ \varepsilon_r \\ \gamma_{\theta r} \\ \gamma_{xr} \\ \gamma_{x\theta} \end{Bmatrix} = \begin{bmatrix} 0 & 0 & 0 \\ 0 & (\partial_\theta/r) & (1/r) \\ 0 & 0 & \partial_r \\ 0 & (\partial_r - 1/r) & (\partial_\theta/r) \\ \partial_r & 0 & 0 \\ (\partial_\theta/r) & 0 & 0 \end{bmatrix} \begin{Bmatrix} u_x \\ u_\theta \\ u_r \end{Bmatrix}, \tag{3}$$

in which u_x,u_θ and u_r are the displacement components; $\partial_i = \partial/\partial i$ $(i = \theta, r)$.

The stress equilibrium equations without body forces are given by

$$\tau_{x\theta,\theta} + \tau_{xr} + r\tau_{xr,r} = 0, \tag{4}$$

$$\sigma_{\theta,\theta} + r\tau_{\theta r,r} + 2\tau_{\theta r} = 0, \tag{5}$$

$$\tau_{\theta r,\theta} + r\sigma_{r,r} + \sigma_r - \sigma_\theta = 0. \tag{6}$$

The charge equation of the FG piezoelectric material without electric charge density is

$$\nabla \cdot \mathbf{D} = 0, \tag{7}$$

where ∇ stands for the del operator, the symbol of $\cdot$ denotes the inner product of vectors and $\mathbf{D}$ is the electric displacement vector.

The relations between the electric field and electric potential are

$$\mathbf{E} = -\nabla\Phi, \tag{8}$$

where $\mathbf{E}$ denotes the electric field vector and Φ is the electric potential.

The boundary conditions of the problem are specified as follows:

On the lateral surfaces the transverse load $\bar{q}_r^{\pm}(\theta)$ and normal electric displacement $\bar{D}_r^{\pm}(\theta)$ (or electric potential $\bar{\Phi}^{\pm}(\theta)$) are prescribed,

$$[\,\tau_{xr} \quad \tau_{\theta r} \quad \sigma_r\,] = [\,0 \quad 0 \quad \bar{q}_r^{\pm}(\theta)\,] \quad \text{on } r = R \pm h, \tag{9}$$

$$\text{either } D_r = \bar{D}_r^{\pm}(\theta) \text{ or } \Phi = \overline{\Phi}^{\pm}(\theta) \quad \text{on } r = R \pm h. \tag{10}$$

The edge boundary conditions for the suitably grounded, simply supported shells (Fig. 1) are

$$\sigma_\theta = u_x = u_r = \Phi = 0 \quad \text{at } \theta = 0 \text{ and } \theta = \theta_\alpha, \tag{11}$$

where θ_α denotes the angle between two edges.

According to Eqs. (1)–(8), it is listed that there are 22 basic equations of the 3D piezoelectricity. For a 3D analysis, we must determine the aforementioned 22 unknown variables satisfying the basic equations (Eqs. (1)–(8)) in the shell domain, the boundary conditions at outer surfaces (Eqs. (9) and (10)) and at the edges (Eq. (11)). Apart from the existingly analytical approaches, we aim at developing the asymptotic formulations for the 3D analysis of FG piezoelectric cylindrical shells under two different electric loads (i.e., prescribed normal electric displacement cases and prescribed electric potential cases).

3. Nondimensionalization

A set of dimensionless coordinates and elastic field variables are defined as

$$\begin{aligned}
&x_1 = x/R \in, \quad x_2 = \theta/\in, \quad x_3 = \zeta/h \text{ and } r = R + \zeta;\\
&u_1 = u_x/R \in, \quad u_2 = u_\theta/R \in, \quad u_3 = u_r/R;\\
&\sigma_1 = \sigma_x/Q, \quad \sigma_2 = \sigma_\theta/Q, \quad \tau_{12} = \tau_{x\theta}/Q;\\
&\tau_{13} = \tau_{xr}/Q \in, \quad \tau_{23} = \tau_{\theta r}/Q \in, \quad \sigma_3 = \sigma_r/Q\in^2;
\end{aligned} \tag{12a–d}$$

where $\in^2 = h/R$; Q denotes a reference elastic moduli.

Two different sets of dimensionless electric field variables are defined as

$$\begin{aligned}
&D_1 = D_x/\in^{(j-1)}e, \quad D_2 = D_\theta/\in^{(j-1)}e, \quad D_3 = D_r/e;\\
&\phi = \Phi e/\in^j RQ;
\end{aligned} \tag{13a–b}$$

where e denotes a reference piezoelectric moduli. In the present formulations, the superscript j is taken as zero that corresponds to the analysis where the normal electric displacement and mechanical load are prescribed on the lateral surfaces; whereas $j = 2$ corresponds to the analysis where the electric potential and mechanical load are prescribed on the lateral surfaces.

To simplify the manipulation of the whole mathematic system, we select transverse stresses (τ_{xr},$\tau_{\theta r}$, σ_r), elastic displacements (u_x, u_θ, u_r), normal electric displacement (D_r) and electric potential (Φ) as primary field variables. The other variables are secondary field variables and can be expressed in terms of primary field variables.

By eliminating the secondary field variables from Eqs. (1)–(8), and then introducing the set of dimensionless coordinates and variables (Eqs. (12) and (13)) in the resulting equations, we can rewrite the basic equations in the form of:

$$u_{3,3} = -\epsilon^2 \bar{a}_2 u_{2,2} - \epsilon^2 \bar{a}_2 u_3 + \epsilon^4 \tilde{\eta}\sigma_3 + \epsilon^2 \tilde{e} D_3, \tag{14}$$

$$u_{1,3} = \epsilon^2 \tilde{s}_{55}\tau_{13}, \tag{15}$$

$$u_{2,3} = -u_{3,2} + \epsilon^2(1 - x_3\partial_3)u_2 + \epsilon^2 \tilde{s}_{44}\tau_{23} + \epsilon^4(x_3\tilde{s}_{44})\tau_{23} - \epsilon^j(\tilde{s}_{44}\tilde{e}_{24})\phi_{,2}, \tag{16}$$

$$D_{3,3} = -\epsilon^j D_{2,2} - \epsilon^2(1 + x_3\partial_3)D_3, \tag{17}$$

$$\tau_{13,3} = -\bar{Q}_{66}u_{1,22} - \epsilon^2(1 + x_3\partial_3)\tau_{13}, \tag{18}$$

$$\tau_{23,3} = -\bar{Q}_{22}u_{2,22} - \bar{Q}_{22}u_{3,2} - \epsilon^2(2 + x_3\partial_3)\tau_{23} - \epsilon^2\tilde{a}_2\sigma_{3,2} - \tilde{b}_2 D_{3,2}, \tag{19}$$

$$\sigma_{3,3} = \bar{Q}_{22}u_{2,2} + \bar{Q}_{22}u_3 - \tau_{23,2} - \epsilon^2(-\tilde{a}_2 + 1 + x_3\partial_3)\sigma_3 + \tilde{b}_2 D_3, \tag{20}$$

$$\phi_{,3} = -\epsilon^{(2-j)}\bar{b}_2 u_{2,2} - \epsilon^{(2-j)}\bar{b}_2 u_3 + \epsilon^{(4-j)}\tilde{e}\sigma_3 - \epsilon^{(2-j)}\tilde{c}D_3, \tag{21}$$

where the superscript j in Eqs. (16), (17) and (21) represents two different electric loading cases, namely the prescribed normal electric displacement cases ($j = 0$) and prescribed electric potential cases ($j = 2$). In addition,

$$[\hat{a}_i \quad \tilde{a}_i \quad \bar{a}_i]^{\mathrm{T}} = \left(\frac{e_{33}e_{3i} + \eta_{33}c_{i3}}{e_{33}^2 + \eta_{33}c_{33}}\right)[\gamma_\theta \quad 1 \quad 1/\gamma_\theta]^{\mathrm{T}}, \quad \gamma_\theta = 1 + \epsilon^2 x_3,$$

$$[\hat{b}_i \quad \tilde{b}_i \quad \bar{b}_i]^{\mathrm{T}} = \left(\frac{e_{33}c_{i3} - c_{33}e_{3i}}{e_{33}^2 + \eta_{33}c_{33}}\right)\left(\frac{e}{Q}\right)[\gamma_\theta \quad 1 \quad 1/\gamma_\theta]^{\mathrm{T}}, \quad \tilde{s}_{55} = \frac{Q}{c_{55}}, \quad \tilde{s}_{44} = \frac{Q}{c_{44}},$$

$$\tilde{e}_{ij} = \frac{e_{ij}}{e}, \quad \tilde{\eta} = \frac{\eta_{33}Q}{e_{33}^2 + \eta_{33}c_{33}}, \quad \tilde{e} = \frac{e_{33}e}{e_{33}^2 + \eta_{33}c_{33}}, \quad \tilde{c} = \frac{c_{33}e^2}{(e_{33}^2 + \eta_{33}c_{33})Q},$$

$$[\hat{Q}_{ij} \quad \tilde{Q}_{ij} \quad \bar{Q}_{ij}]^{\mathrm{T}} = (Q_{ij}/Q)[\gamma_\theta \quad 1 \quad 1/\gamma_\theta]^{\mathrm{T}} \text{ and } Q_{ij} = c_{ij} - \tilde{a}_j c_{i3} - (\tilde{b}_j Q/e)e_{3i}.$$

The secondary field variables, such as in-surface stresses and electric displacements, can be expressed in terms of the primary variables as follows:

$$\sigma_1 = \bar{Q}_{12}u_{2,2} + \bar{Q}_{12}u_3 + \epsilon^2\tilde{a}_1\sigma_3 + \tilde{b}_1 D_3, \tag{22}$$

$$\sigma_2 = \bar{Q}_{22}u_{2,2} + \bar{Q}_{22}u_3 + \epsilon^2\tilde{a}_2\sigma_3 + \tilde{b}_2 D_3, \tag{23}$$

$$\tau_{12} = \bar{Q}_{66}u_{1,2}, \tag{24}$$

$$D_1 = \epsilon^{(2-j)}\tilde{s}_{55}\tilde{e}_{15}\tau_{13}, \tag{25}$$

$$D_2 = \epsilon^{(2-j)}\tilde{s}_{44}\tilde{e}_{24}\tau_{23} - \left[\left(\tilde{s}_{44}\tilde{e}_{24}^2 + \frac{\eta_{22}Q}{e^2}\right)\Big/\gamma_\theta\right]\phi_{,2}. \tag{26}$$

The dimensionless form of boundary conditions of the problem are given as follows:

On the lateral surface the transverse load and normal electric displacement are prescribed,

$$[\tau_{13} \quad \tau_{23} \quad \sigma_3] = [0 \quad 0 \quad \bar{q}_3^{\pm}(x_2)] \quad \text{on } x_3 = \pm 1, \tag{27}$$

$$\text{either } D_3 = \bar{D}_3^{\pm}(x_2) \quad \text{on } x_3 = \pm 1 (j = 0), \text{ or } \phi = \overline{\phi}^{\pm}(x_2) \quad \text{on } x_3 = \pm 1 (j = 2), \tag{28}$$

where $\bar{q}_3^{\pm} = \bar{q}_r^{\pm}/Q\epsilon^2$; $\bar{D}_3^{\pm} = \bar{D}_r^{\pm}/e$; $\overline{\phi}^{\pm} = \overline{\Phi}^{\pm}e/\epsilon^2 RQ$.

At the edges, the following quantities are satisfied:

$$\sigma_1 = u_1 = u_3 = \phi = 0 \text{ at } x_2 = 0 \text{ and } x_2 = \theta_\alpha/\sqrt{h/R}. \tag{29}$$

4. Asymptotic expansions

Since Eqs. (14)–(21) contain terms involving only even powers of ϵ, we therefore asymptotically expand the primary variables in the powers ϵ^2 as given by

$$f(x_2, x_3, \epsilon) = f^{(0)}(x_2, x_3) + \epsilon^2 f^{(1)}(x_2, x_3) + \epsilon^4 f^{(2)}(x_2, x_3) + \cdots. \tag{30}$$

4.1. Prescribed normal electric displacement cases ($j = 0$)

Substituting Eq. (30) into Eqs. (14)–(21), letting $j = 0$ and collecting coefficients of equal powers of ϵ, we obtain the following sets of recurrence equations for various order problems.

4.1.1. The leading-order problem

After performing nondimensionalization and asymptotic expansion manipulation, we obtain the basic differential equations for the leading-order problem given by

$$u_3^{(0)},_3 = 0, \tag{31}$$

$$\phi^{(0)},_3 = 0, \tag{32}$$

$$u_1^{(0)},_3 = 0, \tag{33}$$

$$u_2^{(0)},_3 = -u_3^{(0)},_2 - (\tilde{s}_{44}\tilde{e}_{24})\phi^{(0)},_2, \tag{34}$$

$$D_3^{(0)},_3 = -D_2^{(0)},_2 = \left[\left(\tilde{s}_{44}\tilde{e}_{24}^2 + \frac{\eta_{22}Q}{e^2}\right)/\gamma_\theta\right]\phi^{(0)},_{22}, \tag{35}$$

$$\tau_{13}^{(0)},_3 = -\overline{Q}_{66}u_1^{(0)},_{22}, \tag{36}$$

$$\tau_{23}^{(0)},_3 = -\overline{Q}_{22}u_2^{(0)},_{22} - \overline{Q}_{22}u_3^{(0)},_2 - \tilde{b}_2 D_3^{(0)},_2, \tag{37}$$

$$\sigma_3^{(0)},_3 = \overline{Q}_{22}u_2^{(0)},_2 + \overline{Q}_{22}u_3^{(0)} - \tau_{23}^{(0)},_2 + \tilde{b}_2 D_3^{(0)}. \tag{38}$$

The transverse loads and normal electric displacement at the lateral surfaces are given as

$$[\,\tau_{13}^{(0)} \quad \tau_{23}^{(0)} \quad \tau_3^{(0)}\,] = [\,0 \quad 0 \quad \overline{q}_3^{\pm}\,] \quad \text{on } x_3 = \pm 1, \tag{39}$$

$$D_3^{(0)} = \overline{D}_3^{\pm}(x_2) \quad \text{on } x_3 = \pm 1. \tag{40}$$

At the edges, the following quantities are satisfied:

$$\sigma_2^{(0)} = u_1^{(0)} = u_3^{(0)} = \phi^{(0)} = 0 \quad \text{at } x_2 = 0 \text{ and } x_2 = \theta_\alpha/\sqrt{h/R}. \tag{41}$$

4.1.2. The higher-order problems

The basic differential equations for the higher-order problems are obtained and given by

$$u_3^{(k)},_3 = -\overline{a}_2 u_2^{(k-1)},_2 - \overline{a}_2 u_3^{(k-1)} + \tilde{e}D_3^{(k-1)} + \tilde{\eta}\sigma_3^{(k-2)}, \tag{42}$$

$$\phi^{(k)},_3 = -\overline{b}_2 u_2^{(k-1)},_2 - \overline{b}_2 u_3^{(k-1)} - \tilde{c}D_3^{(k-1)} + \tilde{e}\sigma_3^{(k-2)}, \tag{43}$$

$$u_1^{(k)},_3 = \tilde{s}_{55}\tau_{13}^{(k-1)}, \tag{44}$$

$$u_2^{(k)},_3 = -u_3^{(k)},_2 - (\tilde{s}_{44}\tilde{e}_{24})\phi^{(k)},_2 + (1 - x_3\partial_3)u_2^{(k-1)} + \tilde{s}_{44}\tau_{23}^{(k-1)} + (x_3\tilde{s}_{44})\tau_{23}^{(k-2)}, \tag{45}$$

$$\begin{aligned} D_3^{(k)},_3 &= -D_2^{(k)},_2 - (1 + x_3\partial_3)D_3^{(k-1)} \\ &= \left[\left(\tilde{s}_{44}\tilde{e}_{24}^2 + \frac{\eta_{22}Q}{e^2}\right)\Big/\gamma_\theta\right]\phi^{(k)},_{22} - (\tilde{s}_{44}\tilde{e}_{24})\tau_{23}^{(k-1)},_2 - (1 + x_3\partial_3)D_3^{(k-1)}, \end{aligned} \tag{46}$$

$$\tau_{13}^{(k)},_3 = -\overline{Q}_{66}u_1^{(k)},_{22} - (1 + x_3\partial_3)\tau_{13}^{(k-1)}, \tag{47}$$

$$\tau_{23}^{(k)},_3 = -\overline{Q}_{22}u_2^{(k)},_{22} - \overline{Q}_{22}u_3^{(k)},_2 - \tilde{b}_2 D_3^{(k)},_2 - (2 + x_3\partial_3)\tau_{23}^{(k-1)} - \tilde{a}_2\sigma_3^{(k-1)},_2, \tag{48}$$

$$\sigma_3^{(k)},_3 = \overline{Q}_{22}u_2^{(k)},_2 + \overline{Q}_{22}u_3^{(k)} - \tau_{23}^{(k)},_2 + \tilde{b}_2 D_3^{(k)} - (-\tilde{a}_2 + 1 + x_3\partial_3)\sigma_3^{(k-1)}. \tag{49}$$

The transverse loads and electric normal displacement at the lateral surfaces are given as

$$[\,\tau_{13}^{(k)} \quad \tau_{23}^{(k)} \quad \tau_3^{(k)}\,] = [\,0 \quad 0 \quad 0\,] \quad \text{on } x_3 = \pm 1, \tag{50}$$

$$D_3^{(k)} = 0 \quad \text{on } x_3 = \pm 1. \tag{51}$$

At the edges, the following quantities are satisfied:

$$\sigma_2^{(k)} = u_1^{(k)} = u_3^{(k)} = \phi^{(k)} = 0 \quad \text{at } x_2 = 0 \text{ and } x_2 = \theta_\alpha/\sqrt{h/R}. \tag{52}$$

It is noted that the secondary variables for various orders can be expressed in terms of the primary variables of lower-order using Eqs. (22)–(26) with $j = 0$. For brevity, these expressions are omitted.

4.2. Prescribed electric potential cases ($j = 2$)

Substituting Eq. (30) into Eqs. (14)–(21), letting $j = 2$ and collecting coefficients of equal powers of ϵ, we obtain the following sets of recurrence equations corresponding to various order problems.

4.2.1. The leading order problem

The basic differential equations for the leading-order problem given by

$$\phi^{(0)}{}_{,3} = -\overline{b}_2 u_2^{(0)}{}_{,2} - \bar{b}_2 u_3^{(0)} - \tilde{c} D_3^{(0)}, \tag{53}$$

$$u_2^{(0)}{}_{,3} = -u_3^{(0)}{}_{,2}, \tag{54}$$

$$D_3^{(0)}{}_{,3} = 0; \tag{55}$$

The other basic equations related to the first derivative of primary field variables $(u_1^{(0)}, u_3^{(0)}, \tau_{13}^{(0)}, \tau_{23}^{(0)}, \sigma_3^{(0)})$ with respect to the thickness coordinate remain identical to those equations in the cases of prescribed normal electric displacement (i.e., Eqs. (31), (33) and (36)–(38)).

The prescribed transverse loads on the lateral surfaces are expressed in the same form as Eq. (39). In addition, electric potential is prescribed as

$$\phi^{(0)} = \overline{\phi}^{\pm}(x_2) \quad \text{on } x_3 = \pm 1. \tag{56}$$

The edge conditions remain the same as those in the cases of prescribed normal electric displacement (Eq. (41)).

4.2.2. The higher-order problems

The basic differential equations for the higher-order problems are obtained and given by

$$\phi^{(k)}{}_{,3} = -\bar{b}_2 u_2^{(k)}{}_{,2} - \bar{b}_2 u_3^{(k)} - \tilde{c} D_3^{(k)} + \tilde{e}\sigma_3^{(k-1)}, \tag{57}$$

$$u_2^{(k)}{}_{,3} = -u_3^{(k)}{}_{,2} - (\tilde{s}_{44}\tilde{e}_{24})\phi^{(k-1)}{}_{,2} + (1 - x_3\partial_3)u_2^{(k-1)} + \tilde{s}_{44}\tau_{23}^{(k-1)} + (x_3\tilde{s}_{44})\tau_{23}^{(k-2)}, \tag{58}$$

$$\begin{aligned} D_3^{(k)}{}_{,3} &= -D_2^{(k-1)}{}_{,2} - (1 + x_3\partial_3)D_3^{(k-1)} \\ &= -\tilde{s}_{44}\tilde{e}_{24}\tau_{23}^{(k-1)}{}_{,2} + \left[\left(\tilde{s}_{44}\tilde{e}_{24}^2 + \frac{\eta_{22}Q}{e^2}\right)\Big/\gamma_\theta\right]\phi^{(k-1)}{}_{,22} - (1 + x_3\partial_3)D_3^{(k-1)}; \end{aligned} \tag{59}$$

The other differential equations are the same as Eqs. (42), (44) and (47)–(49).

The prescribed transverse loads on the lateral surfaces are in the same form as Eq. (50) and the electric potential is given as

$$\phi^{(k)} = 0 \quad \text{on } x_3 = \pm 1. \tag{60}$$

The edge conditions remain the same as those in the cases of prescribed normal electric displacement (Eq. (52)).

Again, the secondary variables for various orders can be expressed in terms of the primary variables of lower-order using Eqs. (22)–(26) with $j = 2$.

5. Successive integration

5.1. Prescribed normal electric displacement cases ($j = 0$)

5.1.1. The leading-order problem

Examination of the sets of asymptotic equations, it is found that the analysis can be carried on by integrating those equations through the thickness direction. We therefore integrate Eqs. (31)–(34) to obtain

$$u_3^{(0)} = u_3^0(x_2), \tag{61}$$

$$\phi^{(0)} = \phi^0(x_2), \tag{62}$$

$$u_1^{(0)} = u_1^0(x_2), \tag{63}$$

$$u_2^{(0)} = u_2^0(x_2) - x_3 u_3^0{}_{,2} - \tilde{E}_{00}^{24}(x_3)\phi^0{}_{,2}, \tag{64}$$

where u_1^0, u_2^0, u_3^0 and ϕ^0 represent the displacements and electric potential on the middle surface; $\tilde{E}_{00}^{kl}(x_3) = \int_0^{x_3} (\tilde{s}_{ll}\tilde{e}_{kl})\,\mathrm{d}\eta$.

By observation from Eq. (64), it is noted that the in-surface displacement at the leading-order level is dependent on the electric potential. Based on the previous study, we may consider Eqs. (61)–(64) as the generalized kinematics assumptions for the cylindrical bending analysis of thin piezoelectric shells under prescribed normal electric displacement.

Proceeding to derive the governing equations for the leading-order, we successively integrate Eqs. (35)–(38) through the thickness with using the lateral boundary conditions on $x_3 = -1$ (Eqs. (39) and (40)) to yield

$$\begin{aligned} D_3^{(0)} &= \overline{D}_3^- + \left[\int_{-1}^{x_3} \left(\tilde{s}_{44}\tilde{e}_{24}^2 + \frac{\eta_{22}Q}{e^2}\right)\left(\frac{1}{\gamma_\theta}\right)\mathrm{d}\eta\right]\phi^0{}_{,22} \\ &= \overline{D}_3^- + D_3^0 \end{aligned} \tag{65}$$

$$\tau_{13}^{(0)} = -\left(\int_{-1}^{x_3} \overline{Q}_{66}\,\mathrm{d}\eta\right)u_1^0{}_{,22}, \tag{66}$$

$$\tau_{23}^{(0)} = -\int_{-1}^{x_3} \left[\overline{Q}_{22}(u_2^0{}_{,22} - \eta u_3^0{}_{,222} - \tilde{E}_{00}^{24}\phi^0{}_{,222}) + \overline{Q}_{22}u_3^0{}_{,2} + \tilde{b}_2(\overline{D}_3^-{}_{,2} + D_3^0{}_{,2})\right]\mathrm{d}\eta, \tag{67}$$

$$\begin{aligned} \sigma_3^{(0)} &= \overline{q}_3^- + \int_{-1}^{x_3} [\overline{Q}_{22}(u_2^0{}_{,2} - \eta u_3^0{}_{,22} - \tilde{E}_{00}^{24}\phi^0{}_{,22}) + \overline{Q}_{22}u_3^0 + \tilde{b}(\overline{D}_3^- + D_3^0)]\mathrm{d}\eta \\ &\quad + \int_{-1}^{x_3} (x_3 - \eta)[\overline{Q}_{22}(u_2^0{}_{,222} - \eta u_3^0{}_{,2222} - \tilde{E}_{00}^{24}\phi^0{}_{,2222}) + \overline{Q}_{22}u_3^0{}_{,22} + \tilde{b}(\overline{D}_3^-{}_{,22} + D_3^0{}_{,22})]\mathrm{d}\eta. \end{aligned} \tag{68}$$

After imposing the lateral boundary conditions on $x_3 = 1$, we obtain the governing equations for the leading order problem as follows:

$$K_{11}u_1^0 = 0, \tag{69}$$

$$K_{22}u_2^0 + K_{23}u_3^0 + K_{24}\phi^0 = \tilde{F}_{32}\overline{D}_3^-{}_{,2}, \tag{70}$$

$$K_{32}u_2^0 + K_{33}u_3^0 + K_{34}\phi^0 = \overline{q}_3^+ - \overline{q}_3^- - \tilde{F}_{32}\overline{D}_3^- + \tilde{H}_{32}\overline{D}_3^-{}_{,22}, \tag{71}$$

$$K_{44}\phi^0 = \overline{D}_3^+ - \overline{D}_3^-, \tag{72}$$

in which

$$\begin{aligned} K_{11} &= -\overline{A}_{66}\partial_{22}, \\ K_{22} &= -\overline{A}_{22}\partial_{22}, \\ K_{23} &= \overline{B}_{22}\partial_{222} - \overline{A}_{22}\partial_2, \\ K_{24} &= (\overline{E}_{22}^{24} - \tilde{F}_{32}^{24})\partial_{222}, \\ K_{32} &= -\overline{B}_{22}\partial_{222} + \overline{A}_{22}\partial_2, \\ K_{33} &= \overline{D}_{22}\partial_{2222} - 2\overline{B}_{22}\partial_{22} + \overline{A}_{22}, \\ K_{34} &= (\overline{G}_{22}^{24} - \tilde{H}_{32}^{24})\partial_{2222} - (\overline{E}_{22}^{24} - \tilde{F}_{32}^{24})\partial_{22}, \\ K_{44} &= \overline{F}^{24}\partial_{22}; \end{aligned}$$

$$\begin{bmatrix} \hat{A}_{ij} \\ \tilde{A}_{ij} \\ \overline{A}_{ij} \end{bmatrix} = \int_{-1}^{1} \begin{bmatrix} \hat{Q}_{ij} \\ \tilde{Q}_{ij} \\ \overline{Q}_{ij} \end{bmatrix} \mathrm{d}x_3, \quad \begin{bmatrix} \hat{B}_{ij} \\ \tilde{B}_{ij} \\ \overline{B}_{ij} \end{bmatrix} = \int_{-1}^{1} x_3 \begin{bmatrix} \hat{Q}_{ij} \\ \tilde{Q}_{ij} \\ \overline{Q}_{ij} \end{bmatrix} \mathrm{d}x_3,$$

$$\begin{bmatrix}\hat{D}_{ij}\\ \tilde{D}_{ij}\\ \overline{D}_{ij}\end{bmatrix}=\int_{-1}^{1}x_3^2\begin{bmatrix}\hat{Q}_{ij}\\ \tilde{Q}_{ij}\\ \overline{Q}_{ij}\end{bmatrix}\mathrm{d}x_3,\quad \begin{bmatrix}\hat{E}_{ij}^{kl}\\ \tilde{E}_{ij}^{kl}\\ \overline{E}_{ij}^{kl}\end{bmatrix}=\int_{-1}^{1}\begin{bmatrix}\hat{Q}_{ij}\\ \tilde{Q}_{ij}\\ \overline{Q}_{ij}\end{bmatrix}\int_0^{x_3}(\tilde{s}_{ll}\tilde{e}_{kl})\mathrm{d}\eta\mathrm{d}x_3,$$

$$\begin{bmatrix}\hat{F}_{3i}^{24}\\ \tilde{F}_{3i}^{24}\\ \overline{F}_{3i}^{24}\end{bmatrix}=\int_{-1}^{1}\begin{bmatrix}\hat{b}_i\\ \tilde{b}_i\\ \overline{b}_i\end{bmatrix}\int_{-1}^{x_3}\left(\frac{1}{\gamma_\theta}\right)\left(\tilde{s}_{44}\tilde{e}_{24}^2+\frac{\eta_{22}Q}{e^2}\right)\mathrm{d}\eta\mathrm{d}x_3,\quad \begin{bmatrix}\hat{F}_{3i}\\ \tilde{F}_{3i}\\ \overline{F}_{3i}\end{bmatrix}=\int_{-1}^{1}\begin{bmatrix}\hat{b}_i\\ \tilde{b}_i\\ \overline{b}_i\end{bmatrix}\mathrm{d}x_3,$$

$$\begin{bmatrix}\hat{F}^{kl}\\ \tilde{F}^{kl}\\ \overline{F}^{kl}\end{bmatrix}=\int_{-1}^{1}\left(\tilde{s}_{ll}\tilde{e}_{kl}^2+\frac{\eta_{kk}Q}{e^2}\right)\begin{bmatrix}\gamma_\theta\\ 1\\ 1/\gamma_\theta\end{bmatrix}\mathrm{d}x_3,\quad \begin{bmatrix}\hat{G}_{ij}^{kl}\\ \tilde{G}_{ij}^{kl}\\ \overline{G}_{ij}^{kl}\end{bmatrix}=\int_{-1}^{1}x_3\begin{bmatrix}\hat{Q}_{ij}\\ \tilde{Q}_{ij}\\ \overline{Q}_{ij}\end{bmatrix}\int_0^{x_3}(\tilde{s}_{ll}\tilde{e}_{kl})\mathrm{d}\eta\mathrm{d}x_3,$$

$$\begin{bmatrix}\hat{H}_{3i}^{24}\\ \tilde{H}_{3i}^{24}\\ \overline{H}_{3i}^{24}\end{bmatrix}=\int_{-1}^{1}x_3\begin{bmatrix}\hat{b}_i\\ \tilde{b}_i\\ \overline{b}_i\end{bmatrix}\int_{-1}^{x_3}\left(\frac{1}{\gamma_\theta}\right)\left(\tilde{s}_{44}\tilde{e}_{24}^2+\frac{\eta_{22}Q}{e^2}\right)\mathrm{d}\eta\mathrm{d}x_3,\quad \begin{bmatrix}\hat{H}_{3i}\\ \tilde{H}_{3i}\\ \overline{H}_{3i}\end{bmatrix}=\int_{-1}^{1}x_3\begin{bmatrix}\hat{b}_i\\ \tilde{b}_i\\ \overline{b}_i\end{bmatrix}\mathrm{d}x_3.$$

Solutions of Eqs. (69)–(72) must be supplemented with the edge boundary conditions (Eq. (41)) to constitute a well-posed boundary value problem. Once u_1^0, u_2^0, u_3^0 and ϕ^0 are determined, the leading-order solutions of other variables of electric and mechanical fields can be obtained by Eqs. (61)–(68).

5.1.2. The higher-order problems

Proceeding to order $\in^{2k}$ ($k=1$, 2, 3, etc) and integrating Eqs. (42)–(45) through the thickness coordinate, we readily obtain

$$u_3^{(k)}=u_3^k(x_2)+\varphi_{3k}(x_2,x_3), \tag{73}$$

$$\phi^{(k)}=\phi^k(x_2)+\varphi_{4k}(x_2,x_3), \tag{74}$$

$$u_1^{(k)}=u_1^k(x_2), \tag{75}$$

$$u_2^{(k)}=u_2^k(x_2)-x_3u_{3,2}^k-\tilde{E}_{00}^{24}(x_3)\phi_{,2}^k+\varphi_{2k}(x_2,x_3), \tag{76}$$

where u_1^k, u_2^k u_3^k and ϕ^k represent the modifications to the elastic displacements and electric potential on the middle surface; φ_{2k}, φ_{3k} and φ_{4k} are the relevant functions.

After integrating Eqs. (46)–(49) through the thickness with using Eqs. (73)–(76) and the lateral boundary conditions (Eqs. (50) and (51)), we obtain the governing equations for higher-order problems as follows:

$$K_{11}u_1^k=0, \tag{77}$$

$$K_{22}u_2^k+K_{23}u_3^k+K_{24}\phi^k=f_{2k}(x_2,1), \tag{78}$$

$$K_{32}u_2^k+K_{33}u_3^k+K_{34}\phi^k=f_{3k}(x_2,1)+\frac{\partial f_{2k}(x_2,1)}{\partial x_2}, \tag{79}$$

$$K_{44}\phi^k=f_{4k}(x_2,1), \tag{80}$$

where f_{2k}, f_{3k} and f_{4k} are the nonhomogenous terms and they can be calculated from the lower-order solutions.

With the appropriate edge boundary conditions (Eq. (52)), we can readily obtain the higher-order modifications (i.e., u_1^k, u_2^k u_3^k and ϕ^k) using the same solution methodology as used in the leading-order problem. Afterwards, the higher-order modifications of other field variables can be obtained by Eqs. (46)–(49) and Eqs. (73)–(76).

It is noted that the governing equations of higher-order problems are the same as those equations of the leading-order problem except for the nonhomogenous terms. In view of the recursive property, a solution methodology applied for solving the leading-order problem can be repeatedly applied for solving the higher-order problems. Hence, the present asymptotic solutions can be obtained in a hierarchic manner.

5.2. Prescribed electric potential cases ($j = 2$)

5.2.1. The leading-order problem

Following the similar derivation in the previous cases of applied normal electric displacement and performing successive integration to those basic differential equations through the thickness direction (Eqs. (31), (33), (54) and (55)), we obtain

$$u_3^{(0)} = u_3^0(x_2), \tag{81}$$

$$u_1^{(0)} = u_1^0(x_2), \tag{82}$$

$$u_2^{(0)} = u_2^0(x_2) - x_3 u_{3,2}^0, \tag{83}$$

$$D_3^{(0)} = D_3^0(x_2), \tag{84}$$

where u_1^0, u_2^0, u_3^0 and D_3^0 represent the displacements and normal electric displacement on the middle surface.

Eqs. (81)–(84) may be regarded as the generalized kinematics assumptions for the cylindrical bending analysis of thin piezoelectric shells under prescribed electric potential.

By integrating the basic differential equations relative to the transverse stresses (Eqs. (36)–(38)) and electric potential (Eq. (53)) through the thickness and using Eqs. (81)–(84) and the lateral boundary conditions on $x_3 = -1$ (Eqs. (39) and (56)), we obtain

$$\phi^{(0)} = \overline{\phi}^- - \int_{-1}^{x_3} \left[\overline{b}_2 \left(u_{2,2}^0 - \eta u_{3,22}^0 \right) + \overline{b}_2 u_3^0 + \tilde{c} D_3^0 \right] \mathrm{d}\eta, \tag{85}$$

$$\tau_{13}^{(0)} = -\left(\int_{-1}^{x_3} \overline{Q}_{66} \mathrm{d}\eta \right) u_{1,22}^0, \tag{86}$$

$$\tau_{23}^{(0)} = -\int_{-1}^{x_3} \left[\overline{Q}_{22} \left(u_{2,22}^0 - \eta u_{3,222}^0 \right) + \overline{Q}_{22} u_{3,2}^0 + \tilde{b}_2 D_{3,2}^0 \right] \mathrm{d}\eta, \tag{87}$$

$$\begin{aligned} \sigma_3^{(0)} = {} & \bar{q}_3^- + \int_{-1}^{x_3} \left[\overline{Q}_{22} \left(u_{2,2}^0 - \eta u_{3,22}^0 \right) + \overline{Q}_{22} u_3^0 + \tilde{b} D_3^0 \right] \mathrm{d}\eta \\ & + \int_{-1}^{x_3} (x_3 - \eta) \left[\overline{Q}_{22} \left(u_{2,222}^0 - \eta u_{3,2222}^0 \right) + \overline{Q}_{22} u_{3,22}^0 + \tilde{b} D_{3,22}^0 \right] \mathrm{d}\eta. \end{aligned} \tag{88}$$

After imposing the lateral boundary conditions on $x_3 = 1$, we obtain the governing equations for the leading-order problem as follows:

$$K_{11} u_1^0 = 0, \tag{89}$$

$$K_{22} u_2^0 + K_{23} u_3^0 + L_{24} D_3^0 = 0, \tag{90}$$

$$K_{32} u_2^0 + K_{33} u_3^0 + L_{34} D_3^0 = \overline{q}_3^+ - \overline{q}_3^-, \tag{91}$$

$$L_{42} u_2^0 + L_{43} u_3^0 + L_{44} D_3^0 = \overline{\phi}^+ - \overline{\phi}^-, \tag{92}$$

in which K_{ij} are defined as previous in the cases of prescribed normal electric displacement, and

$$L_{24} = -\tilde{F}_{32} \partial_2,$$

$$L_{34} = -\tilde{H}_{32} \partial_{22} + \tilde{F}_{32},$$

$$L_{42} = -\bar{F}_{32} \partial_2,$$

$$L_{43} = \overline{H}_{32} \partial_{22} - \overline{F}_{32},$$

$$L_{44} = -E_0,$$

$$E_0 = \int_{-1}^{1} \tilde{c} \mathrm{d}x_3.$$

Solutions of Eqs. (89)–(92) must be supplemented with the edge boundary conditions (Eq. (41)) to constitute a well-posed boundary value problem. Once u_1^0, u_2^0, u_3^0 and D_3^0 are determined, the leading-order solutions of other variables of electric and mechanical fields can be obtained from Eqs. (81)–(88).

5.2.2. The higher-order problems

Proceeding to order $\in^{2k}$ ($k = 1, 2, 3$, etc.) and integrating Eqs. (42), (44), (58) and (59) through the thickness coordinate, we readily obtain

$$u_3^{(k)} = u_3^k(x_2) + \psi_{3k}(x_2, x_3), \tag{93}$$

$$D_3^{(k)} = D_3^k(x_2) + \psi_{4k}(x_2, x_3), \tag{94}$$

$$u_1^{(k)} = u_1^k(x_2), \tag{95}$$

$$u_2^{(k)} = u_2^k(x_2) - x_3 u_{3,2}^k + \psi_{2k}(x_2, x_3), \tag{96}$$

where u_1^k, u_2^k u_3^k and D_3^k represent the modifications to the elastic displacements and electric potential on the middle surface; ψ_{2k}, ψ_{3k} and ψ_{4k} are the relevant functions.

After integrating the basic differential equations (Eqs. (47)–(49) and (57)) through the thickness with using Eqs. (93)–(96) and the lateral boundary conditions (Eqs. (50) and (60)), we obtain the governing equations for higher-order problems as follows:

$$K_{11} u_1^k = 0, \tag{97}$$

$$K_{22} u_2^k + K_{23} u_3^k + L_{24} \phi^k = g_{2k}(x_2, 1), \tag{98}$$

$$K_{32} u_2^k + K_{33} u_3^k + L_{34} D_3^k = g_{3k}(x_2, 1) + \frac{\partial g_{2k}(x_2, 1)}{\partial x_2}, \tag{99}$$

$$L_{42} u_2^k + L_{43} u_3^k + L_{44} D_3^k = g_{4k}(x_2, 1), \tag{100}$$

where g_{2k}, g_{3k} and g_{4k} are the nonhomogenous terms and they can be calculated from the lower-order solutions.

With the appropriate edge boundary conditions (Eq. (52)), the higher-order modifications (i.e., u_1^k, u_2^k u_3^k and D_3^k) can be readily obtained using the same solution methodology as used in the leading-order problem. Afterwards, the higher-order modifications of other field variables can be obtained from Eqs. (47)–(49), (57) and (93)–(96).

6. Applications to benchmark problems

The benchmark problems of simply-supported, functionally graded piezoelectric cylindrical shells under lateral electromechanical loads (Fig. 2) are studied using the present asymptotic formulations.

The electromechanical loads acting on lateral surface of the shell ($\zeta = h$) are considered and expressed by the Fourier series in the dimensionless form of

$$\overline{q}_r^+(x_2) = \sum_{n=1}^{\infty} \overline{q}_n \sin \tilde{n} x_2, \tag{101}$$

$$\overline{D}_r^+(x_2) = \sum_{n=1}^{\infty} \overline{D}_n \sin \tilde{n} x_2, \tag{102}$$

$$\overline{\phi}^+(x_2) = \sum_{n=1}^{\infty} \overline{\phi}_n \sin \tilde{n} x_2, \tag{103}$$

where $\tilde{n} = n/\sqrt{h/R}$ and n is a positive integer.

The applications of the present asymptotic formulations to various piezoelectric cylindrical shells under previous two cases of electromechanical loads are detailed described as follows.

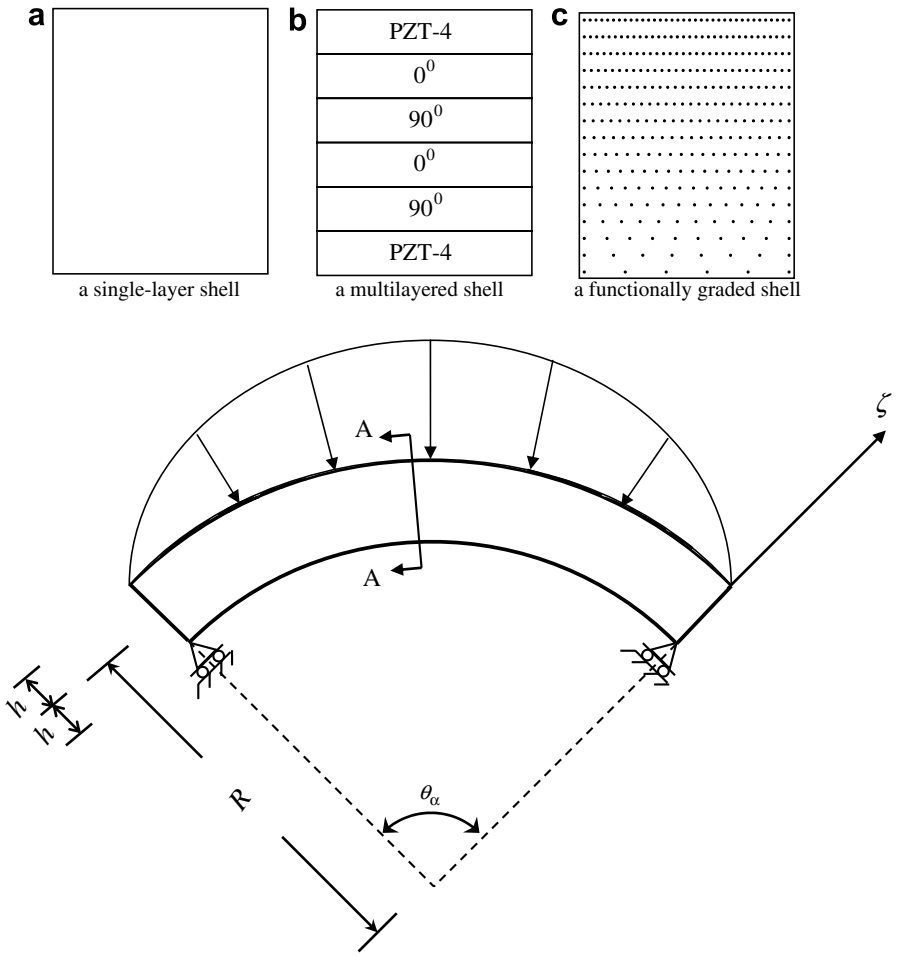

Fig. 2. The geometry and coordinates of a typical cross section of a cylindrical strip.

6.1. Prescribed normal electric displacement cases ($j = 0$)

The governing equations of the leading-order problem (Eqs. (69)–(72)) can be readily solved by letting

$$u_1^0 = \sum_{n=1}^{\infty} u_{1n}^0 \sin \tilde{n} x_2, \tag{104}$$

$$u_2^0 = \sum_{n=1}^{\infty} u_{2n}^0 \cos \tilde{n} x_2, \tag{105}$$

$$u_3^0 = \sum_{n=1}^{\infty} u_{3n}^0 \sin \tilde{n} x_2, \tag{106}$$

$$\phi^0 = \sum_{n=0}^{\infty} \phi_n^0 \sin \tilde{n} x_2. \tag{107}$$

Substituting Eqs. (104)–(107) into Eqs. (69)–(72) gives

$$\begin{bmatrix} k_{11} & 0 & 0 & 0 \\ 0 & k_{22} & k_{23} & k_{24} \\ 0 & k_{32} & k_{33} & k_{34} \\ 0 & 0 & 0 & k_{44} \end{bmatrix} \begin{Bmatrix} u_{1n}^0 \\ u_{2n}^0 \\ u_{3n}^0 \\ \phi_n^0 \end{Bmatrix} = \begin{Bmatrix} 0 \\ 0 \\ \overline{q}_n \\ \overline{D}_n \end{Bmatrix}, \tag{108}$$

where k_{ij} are the relevant coefficients.

The elastic displacement u_{1n}^0 u_{2n}^0, u_{3n}^0 and electric potential ϕ_n^0 can be determined from Eq. (108). Once u_{1n}^0, u_{2n}^0 u_{3n}^0 and ϕ_n^0 are determined, the $\in^0$-order solution can be obtained from Eqs. (61)–(68). The summation signs would be dropped for brevity in the following derivation.

Carrying on the solution to higher-order ($\in^{2k}$-order, $k = 1, 2, 3$, etc.), we find that the nonhomogeneous terms for fixed values of n in the $\in^{2k}$-order equations are

$$f_{2k}(x_2, 1) = \tilde{f}_{2k}(1)\cos\tilde{n}x_2, \tag{109}$$

$$f_{3k}(x_2, 1) = \tilde{f}_{3k}(1)\sin\tilde{n}x_2, \tag{110}$$

$$f_{4k}(x_2, 1) = \tilde{f}_{4k}(1)\sin\tilde{n}x_2. \tag{111}$$

In view of the recurrence of the equations, the $\in^{2k}$-order solution can be obtained by letting

$$u_1^k = u_{1n}^k \sin\tilde{n}x_2, \tag{112}$$

$$u_2^k = u_{2n}^k \cos\tilde{n}x_2, \tag{113}$$

$$u_3^k = u_{3n}^k \sin\tilde{n}x_2, \tag{114}$$

$$\phi^k = \phi_n^k \sin\tilde{n}x_2. \tag{115}$$

Substituting Eqs. (109)–(111) and Eqs. (112)–(115) into Eqs. (77)–(80) gives

$$\begin{bmatrix} k_{11} & 0 & 0 & 0 \\ 0 & k_{22} & k_{23} & k_{24} \\ 0 & k_{32} & k_{33} & k_{34} \\ 0 & 0 & 0 & k_{44} \end{bmatrix} \begin{Bmatrix} u_{1n}^k \\ u_{2n}^k \\ u_{3n}^k \\ \phi_n^k \end{Bmatrix} = \begin{Bmatrix} .0 \\ \tilde{f}_{2k}(1) \\ \tilde{f}_{3k}(1) - \tilde{n}\tilde{f}_{2k}(1) \\ \tilde{f}_{4k}(1) \end{Bmatrix}. \tag{116}$$

Following the similar solution process of the leading-order level, we obtain the modifications of generalized kinematics variables u_{1n}^k, u_{2n}^k, u_{3n}^k and ϕ_n^k for the higher-order problems. Afterwards, the $\in^{2k}$-order corrections are determined using Eqs. (46)–(49) and Eqs. (73)–(76). It is shown that the solution process can be repeatedly applied for various order problems and the asymptotic solutions can be obtained in a hierarchic manner.

6.2. Prescribed electric potential cases ($j = 2$)

The governing equations of the leading-order problem (Eqs. (89)–(92)) can be also solved by letting u_1^0, u_2^0 and u_3^0 be in the same forms as Eqs. (104)–(106) and

$$D_3^0 = \sum_{n=1}^{\infty} D_{3n}^0 \sin\tilde{n}x_2. \tag{117}$$

Substituting Eqs. (104)–(106) and (117) into Eqs. (89)–(92) gives

$$\begin{bmatrix} k_{11} & 0 & 0 & 0 \\ 0 & k_{22} & k_{23} & l_{24} \\ 0 & k_{32} & k_{33} & l_{34} \\ 0 & l_{42} & l_{43} & l_{44} \end{bmatrix} \begin{Bmatrix} u_{1n}^0 \\ u_{2n}^0 \\ u_{3n}^0 \\ D_{3n}^0 \end{Bmatrix} = \begin{Bmatrix} 0 \\ 0 \\ \overline{q}_n \\ \overline{\phi}_n \end{Bmatrix}, \tag{118}$$

where l_{ij} are the relevant coefficients; k_{ij} are the same as those in Eq. (108).

The elastic displacement u_{1n}^0 u_{2n}^0, v_{3n}^0 and electric displacement D_{3n}^0 can be obtained by solving the simultaneously algebraic equations (118). Once they are determined, the $\in^0$-order solution can be obtained from Eqs. (81)–(88). Again, the summation signs would be dropped for brevity in the following derivation.

Carrying on the solution to higher-order ($\in^{2k}$-order, $k = 1, 2, 3$, etc.), we find that the nonhomogeneous terms for fixed values of n in the $\in^{2k}$-order equations are

$$g_{2k}(x_2, 1) = \tilde{g}_{2k}(1)\cos\tilde{n}x_2, \tag{119}$$

$$g_{3k}(x_2, 1) = \tilde{g}_{3k}(1)\sin\tilde{n}x_2, \tag{120}$$

$$g_{4k}(x_2, 1) = \tilde{g}_{4k}(1)\sin\tilde{n}x_2. \tag{121}$$

In view of the recurrence of the equations, the $\in^{2k}$-order solution can be obtained by letting u_1^k, u_2^k and u_3^k be in the same forms as Eqs. (112)–(114) and

$$D_3^k = D_{3n}^k \sin\tilde{n}x_2. \tag{122}$$

Substituting Eqs. (112)–(114) and (122) into Eqs. (97)–(100) gives

$$\begin{bmatrix} k_{11} & 0 & 0 & 0 \\ 0 & k_{22} & k_{23} & l_{24} \\ 0 & k_{32} & k_{33} & l_{34} \\ 0 & l_{42} & l_{43} & l_{44} \end{bmatrix} \begin{Bmatrix} u_{1n}^k \\ u_{2n}^k \\ u_{3n}^k \\ D_{3n}^k \end{Bmatrix} = \begin{Bmatrix} 0 \\ \tilde{g}_{2k}(1) \\ \tilde{g}_{3k}(1) - \tilde{n}\tilde{g}_{2k}(1) \\ \tilde{g}_{4k}(1) \end{Bmatrix}. \tag{123}$$

By solving the system of algebraic equations (123), we may obtain the modifications of generalized kinematics variables u_{1n}^k, u_{2n}^k, u_{3n}^k and D_{3n}^k for the higher-order problems. Afterwards, the $\in^{2k}$-order corrections are determined using Eqs. (47)–(49), (57) and (93)–(96). Again, it is shown that the solution process can be repeatedly applied for various order problems and the asymptotic solutions can be obtained in a hierarchic manner.

7. Illustrative examples

In illustrative examples, we consider four cases of electromechanical loads as follows:

For the cases of prescribed electric potential ($j = 2$), we consider

$$\text{Case 1. } \overline{q}_r^+ = q_0 \sin\left(\frac{\pi}{\theta_\alpha}\theta\right) = \text{N/m}^2,\ \overline{q}_r^- = 0\ \text{N/m}^2;\quad \overline{\Phi}^+ = 0\ \text{V},\ \overline{\Phi}^- = 0\ \text{V}. \tag{124}$$

$$\text{Case 2. } \overline{q}_r^+ = 0\ \text{N/m}^2,\ \overline{q}_r^- = 0\ \text{N/m}^2;\quad \overline{\Phi}^+ = \phi_0 \sin\left(\frac{\pi}{\theta_\alpha}\theta\right)\text{V},\ \overline{\Phi}^- = 0\ \text{V}. \tag{125}$$

For the cases of prescribed normal electric displacement ($j = 0$), we consider

$$\text{Case 3. } \overline{q}_r^+ = q_0 \sin\left(\frac{\pi}{\theta_\alpha}\theta\right) = \text{N/m}^2,\ \overline{q}_r^- = 0\ \text{N/m}^2;\quad \overline{D}_r^+ = 0\ \text{C/m}^2,\ \overline{D}_r^- = 0\ \text{C/m}^2. \tag{126}$$

$$\text{Case 4. } \overline{q}_r^+ = 0\ \text{N/m}^2,\ \overline{q}_r^- = 0\ \text{N/m}^2;\ \overline{D}_r^+ = D_0 \sin\left(\frac{\pi}{\theta_\alpha}\theta\right)\text{C/m}^2,\ \overline{D}_r^- = 0\ \text{C/m}^2. \tag{127}$$

Since the material is considered as heterogeneous through the thickness coordinate in the present asymptotic formulations, we evaluate the structural behavior of two types of piezoelectric cylindrical shells by assuming appropriate material property variations through the thickness coordinate as follows:

Type 1-single-layer piezoelectric cylindrical shells.

For a Type 1 shell, the material properties are assumed as homogeneous, independent upon the thickness coordinate, and are given by

$$m_{ij}(\zeta) = m_{ij}, \tag{128}$$

where $m_{ij} = c_{ij}$, e_{ij} and η_{ij}.

Type 2-functionally graded piezoelectric shells.

For a Type 2 shell, the material properties are assumed to obey the identical exponent-law varied exponentially with the thickness coordinate and are given by

$$m_{ij} = m_{ij}^{(b)} \mathrm{e}^{\alpha[(\zeta+h)/2h]}, \tag{129}$$

where the superscript b in the parentheses denotes the bottom surface; α is the material property gradient index which represents the degree of the material gradient along the thickness and can be determined by the values of the material properties at the top and bottom surfaces, i.e.,

$$\alpha = \ln \frac{m_{ij}^{(t)}}{m_{ij}^{(b)}}, \tag{130}$$

where the superscript t in the parentheses denotes the top surface. $\ln(z)$ denotes the natural logarithm function of z which is the inverse of the exponential function, e^z. A typical exponential function $e^{\alpha[(\zeta+h)/2h]}$ used for material properties in the present analysis, is sketched in Fig. 3 where α is taken as the values of -3.0, -1.5, 0, 1.5, 3, respectively.

7.1. Single-layer piezoelectric cylindrical shells

For comparison purpose, the present asymptotic formulations are applied to the cylindrical bending analysis of simply-supported, single-layer homogeneous piezoelectric cylindrical shells in Tables 2 and 3. The shells are considered to be composed of polyvinyledence fluoride (PVDF) polarized along the radial direction. The elastic, piezoelectric and dielectric properties of PVDF material are given in Table 1. The loading conditions on lateral surfaces are considered as Cases 1 and 2 with $q_0 = -1$ N/m^2 and $\phi_0 = -1$ V (Eqs. (124) and (125)), respectively, in Tables 2 and 3. The dimensionless variables are denoted as the same forms of those in the reference (Dumir et al., 1997). For loading conditions of Case 1 in Table 2 where the mechanical load is applied with free electric potential on the lateral surfaces of the shells, the dimensionless variables are denoted as

$$\begin{aligned}
&(\overline{u}_\theta, \overline{u}_r) = \frac{100 Y_r}{2hS^4|q_0|}(u_\theta, u_r),\\
&(\overline{\sigma}_x, \overline{\sigma}_\theta, \overline{\sigma}_r, \overline{\tau}_{\theta r}) = (\sigma_x/S^2, \sigma_\theta/S^2, \sigma_r, \tau_{\theta r}/S)/|q_0|,\\
&(\overline{D}_\theta, \overline{D}_r) = (D_\theta, D_r)/|d_1|S|q_0|\\
&\overline{\phi} = |d_1|Y_r\phi/2\, hS^2|q_0|,
\end{aligned} \tag{131a–d}$$

and $S = R/2h$, $Y_r = 2.0$ GPa, $d_1 = -30 \times 10^{-12}$CN^{-1}.

For loading conditions of Case 2 in Table 3 where the electric potential is applied with free tractions on the lateral surfaces of the shells, the dimensionless variables are denoted as

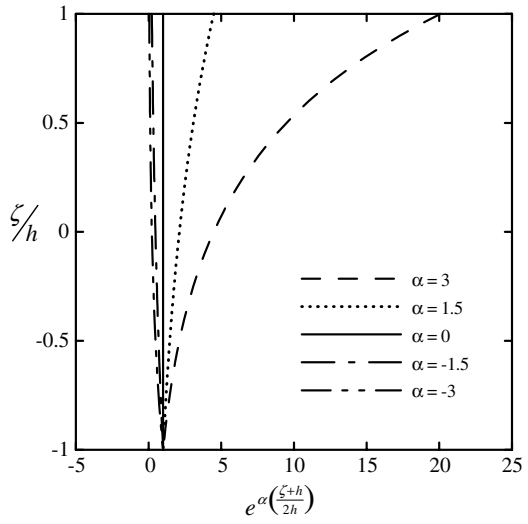

Fig. 3. Variation of normalized material properties along the thickness coordinate in the FG piezoelectric shells.

Table 1
Elastic, piezoelectric and dielectric properties of piezoelectric materials

Moduli	PVDT (Dumir et al., 1997)	PZT-4 (Vel et al., 2004)
c_{11} (GPa)	3.0	138.499
c_{22}	3.0	138.499
c_{33}	3.0	114.745
c_{12}	1.5	77.371
c_{13}	1.5	73.643
c_{23}	1.5	73.643
c_{44}	0.75	25.6
c_{55}	0.75	25.6
c_{66}	0.75	30.6
e_{24} (C/m^2)	0.0	12.72
e_{15}	0.0	12.72
e_{31}	−0.15e−02	−5.2
e_{32}	0.285e−01	−5.2
e_{33}	−0.51e−01	15.08
η_{11} (F/m)	0.1062e−09	1.306e−08
η_{22}	0.1062e−09	1.306e−08
η_{33}	0.1062e−09	1.151e−08

$$(\overline{u}_\theta, \overline{u}_r) = \frac{100}{|d_1|S|\phi_0|}(u_\theta, u_r),$$
$$(\overline{\sigma}_x, \overline{\sigma}_\theta, \overline{\sigma}_r, \overline{\tau}_{\theta r}) = (\sigma_x, S^2\sigma_\theta, S^3\sigma_r, S^3\tau_{\theta r})2h/Y_r|d_1||\phi_0|,$$
$$(\overline{D}_\theta, \overline{D}_r) = (SD_\theta, D_r)2h/|d_1|^2 Y_r|\phi_0|$$
$$\overline{\phi} = \phi/|\phi_0|. \tag{132a–d}$$

Tables 2 and 3 show the present asymptotic solutions of elastic and electric field variables for various orders at crucial positions in the cylindrical shells. The present asymptotic solutions are computed up to the $\in^{12}$-order level with $R/2h = 4$, 10, 100 and $\theta_\alpha = \pi/3$. It is shown that the convergent speed in the cases of thin shells is more rapid than that in the cases of thick shells. The present convergent solutions yield at the $\in^8$-order level for the cases of thick shells ($R/2h = 4$), at the $\in^6$-order level for the cases of moderately thick shells ($R/2h = 10$) and at the $\in^4$-order level for the cases of thin shells ($R/2h = 100$). The present convergent solutions are also compared with the 3D piezoelectricity solutions available in the literature (Dumir et al., 1997). It is shown that the present convergent solutions are in good agreement with the 3D piezoelectricity solutions.

7.2. Functionally graded piezoelectric cylindrical shells

Figs. 4–6 show the variations of mechanical and electric variables across the thickness coordinate for the moderately shells ($R/2h = 10$) under loading conditions of Cases 1, 2 and 4, respectively, where α is taken as −3.0, −1.5, 0, 1.5, 3.0.. The material properties are assumed to obey the identical exponent-law varied exponentially with the thickness coordinate and are given in Eq. (129). The material properties of PZT-4 are used as the reference material properties (Table 1) and placed on the bottom surface (i.e., $c_{ij}^{(b)}, e_{ij}^{(b)}, \eta_{ij}^{(b)}$). According to Eq. (130), the ratio of material properties between top surface and bottom surface is given as

$$\frac{c_{ij}^{(t)}}{c_{ij}^{(b)}} = \frac{e_{ij}^{(t)}}{e_{ij}^{(b)}} = \frac{\eta_{ij}^{(t)}}{\eta_{ij}^{(b)}} = e^{\alpha}, \tag{133}$$

where α is considered to range from −3.0 to 3.0 so that the ratio of material properties between top surface and bottom surface is approximately from 0.05 to 20. In addition, the present results for FG piezoelectric shells with a particular value of $\alpha = 0$ may reduce to the results of single-layer homogeneous piezoelectric shells.

Table 2
Mechanical and electric components at the crucial positions in single-layer piezoelectric cylindrical shells (PVDF) under cylindrical bending (case 1)

$R/2h$	$\in^{2k}$	$\overline{u}_\theta(0,+h)$	$\overline{u}_\theta(0,-h)$	$\overline{u}_r(\frac{\theta_x}{2},0)$	$\overline{\sigma}_x(\frac{\theta_x}{2},+h)$	$\overline{\sigma}_x(\frac{\theta_x}{2},-h)$	$\overline{\sigma}_\theta(\frac{\theta_x}{2},+h)$	$\overline{\sigma}_\theta(\frac{\theta_x}{2},-h)$	$\overline{\sigma_r}(\frac{\theta_x}{2},0)$	$\overline{\tau}_{\theta r}(0,0)$	$10^3\overline{\phi}(\frac{\theta_x}{2},0)$	$10\overline{D}_r(\frac{\theta_x}{2},+h)$	$10\overline{D}_r(\frac{\theta_x}{2},-h)$	$\overline{D}_\theta(0,0)$
4	$\in^0$	0.7432	−8.9744	−12.9568	−0.2058	0.2433	−0.6148	0.7270	0.1499	−0.4992	2.2113	0.0000	0.0000	−0.3914
	$\in^2$	−0.3777	−12.2956	−19.2634	−0.2706	0.3145	−0.7466	0.9399	0.2069	−0.6132	2.4302	0.1164	2.1034	−0.4301
	$\in^4$	−0.7915	−12.9657	−20.7983	−0.2746	0.3244	−0.7585	0.9696	0.2159	−0.6229	2.4399	0.0299	2.5156	−0.4319
	$\in^6$	−0.8675	−13.0728	−21.0594	−0.2749	0.3255	−0.7596	0.9730	0.2169	−0.6237	2.4425	0.0218	2.5472	−0.4323
	$\in^8$	−0.8788	−13.0879	−21.0972	−0.2750	0.3257	−0.7597	0.9734	0.2170	−0.6237	2.4427	0.0214	2.5494	−0.4324
	$\in^{10}$	−0.8804	−13.0899	−21.1022	−0.2750	0.3257	−0.7597	0.9735	0.2170	−0.6238	2.4427	0.0213	2.5496	−0.4324
	$\in^{12}$	−0.8806	−13.0902	−21.1029	−0.2750	0.3257	−0.7597	0.9735	0.2170	−0.6238	2.4428	0.0213	2.5496	−0.4324
	3D solutions (Dumir et al., 1997)	−0.8806	−13.09	−21.10	−0.2750	0.3257	−0.7597	0.9735	0.2170	−0.6238	2.443	0.0213	2.550	−0.4324
10	$\in^0$	−2.3513	−6.2520	−13.0025	−0.2159	0.2308	−0.6451	0.6896	1.1600	−0.4999	2.2142	0.0000	0.0000	−0.3919
	$\in^2$	−3.3276	−7.8519	−16.8350	−0.2510	0.2724	−0.7402	0.8140	1.3886	−0.5798	2.5225	−0.0810	0.7047	−0.4465
	$\in^4$	−3.5329	−8.1285	−17.5532	−0.2544	0.2773	−0.7501	0.8286	1.4161	−0.5882	2.5558	−0.1496	0.7782	−0.4524
	$\in^6$	−3.5665	−8.1702	−17.6658	−0.2547	0.2778	−0.7512	0.8302	1.4191	−0.5891	2.5595	−0.1566	0.7826	−0.4530
	$\in^8$	−3.5715	−8.1761	−17.6819	−0.2548	0.2779	−0.7513	0.8304	0.4195	−0.5892	2.5600	−0.1574	0.7829	−0.4531
	$\in^{10}$	−3.5722	−8.1769	−17.6841	−0.2548	0.2779	−0.7514	0.8304	1.4195	−0.5893	2.5600	−0.1574	0.7830	−0.4531
	$\in^{12}$	−3.5723	−8.1770	−17.6844	−0.2548	0.2779	−0.7514	0.8304	1.4195	−0.5893	2.5600	−0.1575	0.7830	−0.4531
	3D solutions (Dumir et al., 1997)	−3.572	−8.177	−17.68	−0.2548	0.2779	−0.7514	0.8304	1.420	−0.5893	2.560	−0.1575	0.7830	−0.4531
100	$\in^0$	−4.1416	−4.5319	−13.0111	−0.2224	0.2239	−0.6645	0.6689	16.1660	−0.5000	2.2148	0.0000	0.0000	−0.3920
	$\in^2$	−5.1054	−5.5411	−15.9705	−0.2479	0.2502	−0.7405	0.7477	18.0972	−0.5580	2.4714	−0.1759	−0.0975	−0.4374
	$\in^4$	−5.2686	−5.7093	−16.4677	−0.2507	0.2532	−0.7490	0.7565	18.3121	−0.5645	2.5000	−0.2010	−0.1148	−0.4425
	$\in^6$	−5.2930	−5.7342	−16.5416	−0.2510	0.2535	−0.7499	0.7574	18.3359	−0.5652	2.5031	−0.2037	−0.1168	−0.4431
	$\in^8$	−5.2964	−5.7377	−16.5519	−0.2510	0.2535	−0.7500	0.7575	18.3386	−0.5653	2.5035	−0.2041	−0.1170	−0.4431
	$\in^{10}$	−5.2968	−5.7382	−16.5533	−0.2510	0.2535	−0.7500	0.7575	18.3389	−0.5653	2.5035	−0.2041	−0.1171	−0.4431
	$\in^{12}$	−5.2969	−5.7382	−16.5535	−0.2510	0.2535	−0.7500	0.7576	18.3389	−0.5653	2.5035	−0.2041	−0.1171	−0.4431
	3D solutions (Dumir et al., 1997)	−5.297	−5.738	−16.55	−0.2510	0.2535	−0.7500	0.7576	18.34	−0.5653	2.504	−0.2041	−0.1171	−0.4431

Table 3
Mechanical and electric components at the crucial positions in single-layer piezoelectric cylindrical shells (PVDF) under cylindrical bending (case 2)

$R/2h$	$\in^{2k}$	$\overline{u}_\theta(0,+h)$	$\overline{u}_\theta(0,-h)$	$\overline{u}_r(\frac{\theta_z}{2},0)$	$\overline{\sigma}_x(\frac{\theta_z}{2},+h)$	$\overline{\sigma}_x(\frac{\theta_z}{2},-h)$	$\overline{\sigma}_\theta(\frac{\theta_z}{2},+h)$	$\overline{\sigma}_\theta(\frac{\theta_z}{2},0)$	$\overline{\sigma}_\theta(\frac{\theta_z}{2},-h)$	$\overline{\tau}_{\theta r}(0-\frac{h}{2})$	$\overline{\phi}(\frac{\theta_z}{2},0)$	$\overline{D}_r(\frac{\theta_z}{2},+h)$	$\overline{D}_r(\frac{\theta_z}{2},-h)$	$\overline{D}_\theta(0,h)$
4	$\in^0$	−27.0370	−20.3704	8.8889	−0.1000	−0.1000	0.0000	0.0000	0.0000	0.0000	−0.5000	60.2017	60.2017	157.3333
	$\in^2$	−28.6269	−13.6980	12.0040	−0.1318	−0.1364	−1.3132	0.7100	−1.5595	0.4048	−0.4981	62.8177	62.4993	157.3333
	$\in^4$	−28.7444	−13.7686	11.9212	−0.1307	−0.1359	−1.2650	0.6757	−1.5355	0.3935	−0.4978	62.7708	62.4753	157.3333
	$\in^6$	−28.7425	−13.7762	11.8976	−0.1307	−0.1359	−1.2659	0.6767	−1.5358	0.3925	−0.4978	62.7676	62.4760	157.3333
	$\in^8$	−28.7434	−13.7763	11.8957	−0.1307	−0.1359	−1.2662	0.6768	−1.5361	0.3925	−0.4978	62.7679	62.4760	157.3333
	$\in^{10}$	−28.7436	−13.7764	11.8953	−0.1307	−0.1359	−1.2661	0.6768	−1.5361	0.3925	−0.4978	62.7679	62.4760	157.3333
	$\in^{12}$	−28.7436	−13.7764	11.8952	−0.1307	−0.1359	−1.2661	0.6768	−1.5361	0.3925	−0.4978	62.7679	62.4760	157.3333
	3D solutions (Dumir et al., 1997)	−28.74	−13.78	11.90	−0.1307	−0.1359	−1.266	0.6768	−1.536	0.3925	−0.4978	62.77	62.48	157.3
10	$\in^0$	−25.0370	−22.3704	8.8889	−0.1000	−0.1000	0.0000	0.0000	0.0000	0.0000	−0.5000	60.2017	60.2017	168.5714
	$\in^2$	−26.3777	−22.0113	6.6537	−0.1025	−0.1085	−1.3732	0.7096	−1.4705	0.4011	−0.5071	58.9259	62.3782	168.5714
	$\in^4$	−26.4755	−22.0890	6.3729	−0.1024	−0.1086	−1.3443	0.6994	−1.4704	0.3986	−0.5070	58.9648	62.3947	168.5714
	$\in^6$	−26.4850	−22.0989	6.3434	−0.1024	−0.1086	−1.3448	0.6995	−1.4705	0.3984	−0.5070	58.9643	62.3945	168.5714
	$\in^8$	−26.4862	−22.1000	6.3401	−0.1024	−0.1086	−1.3448	0.6995	−1.4705	0.3984	−0.5070	58.9643	62.3945	168.5714
	$\in^{10}$	−26.4863	−22.1001	6.3397	−0.1024	−0.1086	−1.3448	0.6995	−1.4705	0.3984	−0.5070	58.9643	62.3945	168.5714
	$\in^{12}$	−26.4863	−22.1001	6.3397	−0.1024	−0.1086	−1.3448	0.6995	−1.4705	0.3984	−0.5070	58.9643	62.3945	168.5714
	3D solutions (Dumir et al., 1997)	−26.49	−22.10	6.340	−0.1024	0.1086	−1.345	0.6995	−1.410	0.3984	−0.5070	58.96	62.39	168.6
100	$\in^0$	−23.8370	−23.5704	8.8889	−0.1000	−0.1000	0.0000	0.0000	0.0000	0.0000	−0.5000	60.2017	60.2017	176.1194
	$\in^2$	−25.7542	−25.4203	3.2304	−0.0996	−0.1005	−1.4143	0.7096	−1.4240	0.3993	−0.5012	59.9188	60.4943	176.1194
	$\in^4$	−25.9637	−25.6297	2.6016	−0.0996	−0.1005	−1.3971	0.7019	−1.4108	0.3953	−0.5012	59.9193	60.4948	176.1194
	$\in^6$	−25.9870	−25.6530	2.5318	−0.0996	−0.1005	−1.3972	0.7019	−1.4108	0.3953	−0.5012	59.9193	60.4948	176.1194
	$\in^8$	−25.9896	−25.6556	2.5240	−0.0996	−0.1005	−1.3972	0.7019	−1.4108	0.3953	−0.5012	59.9193	60.4948	176.1194
	$\in^{10}$	−25.9898	−25.6559	2.5232	−0.0996	−0.1005	−1.3972	0.7019	−1.4108	0.3953	−0.5012	59.9193	60.4948	176.1194
	$\in^{12}$	−25.9899	−25.6559	2.5231	−0.0996	−0.1005	−1.3972	0.7019	−1.4108	0.3953	−0.5012	59.9193	60.4948	176.1194
	3D solutions (Dumir et al., 1997)	−25.99	−25.66	2.523	−0.0996	−0.1005	−1.397	0.7019	−1.411	0.3953	−0.5012	59.92	60.49	176.1

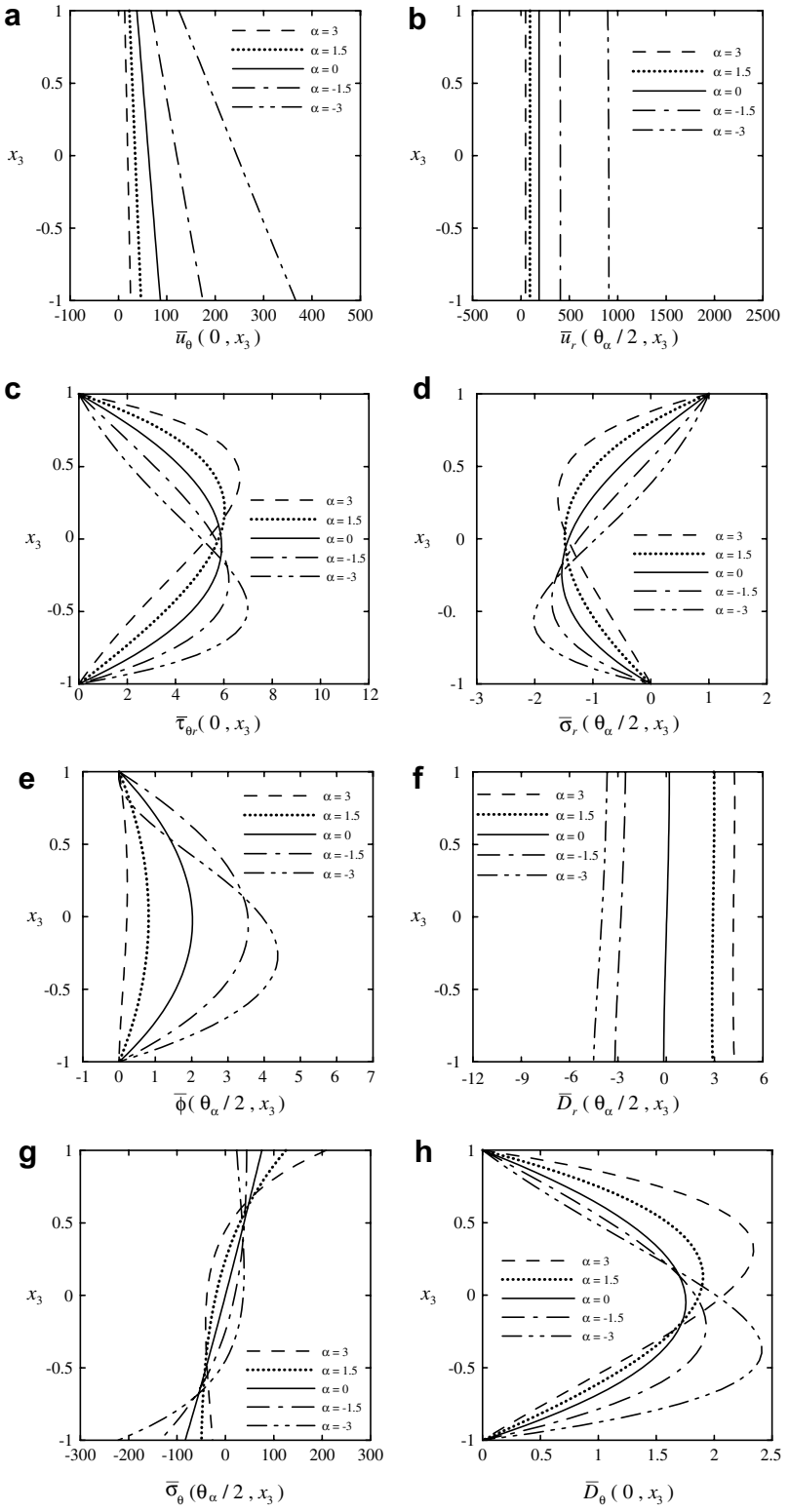

Fig. 4. Distributions of elastic and electric field variables through the thickness of FG piezoelectric cylindrical shell under cylindrical bending (Case 1).

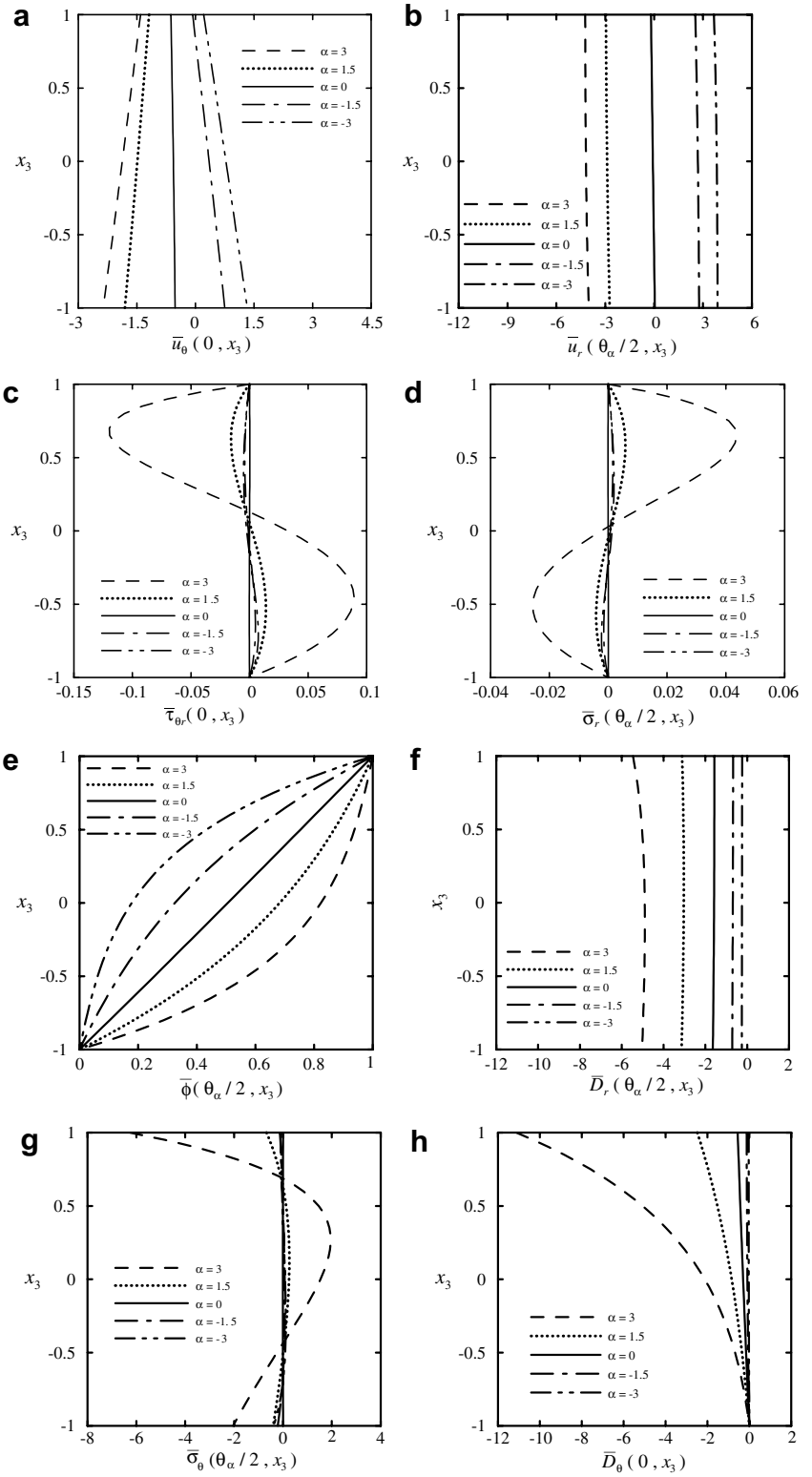

Fig. 5. Distributions of elastic and electric field variables through the thickness of FG piezoelectric cylindrical shell under cylindrical bending (Case 2).

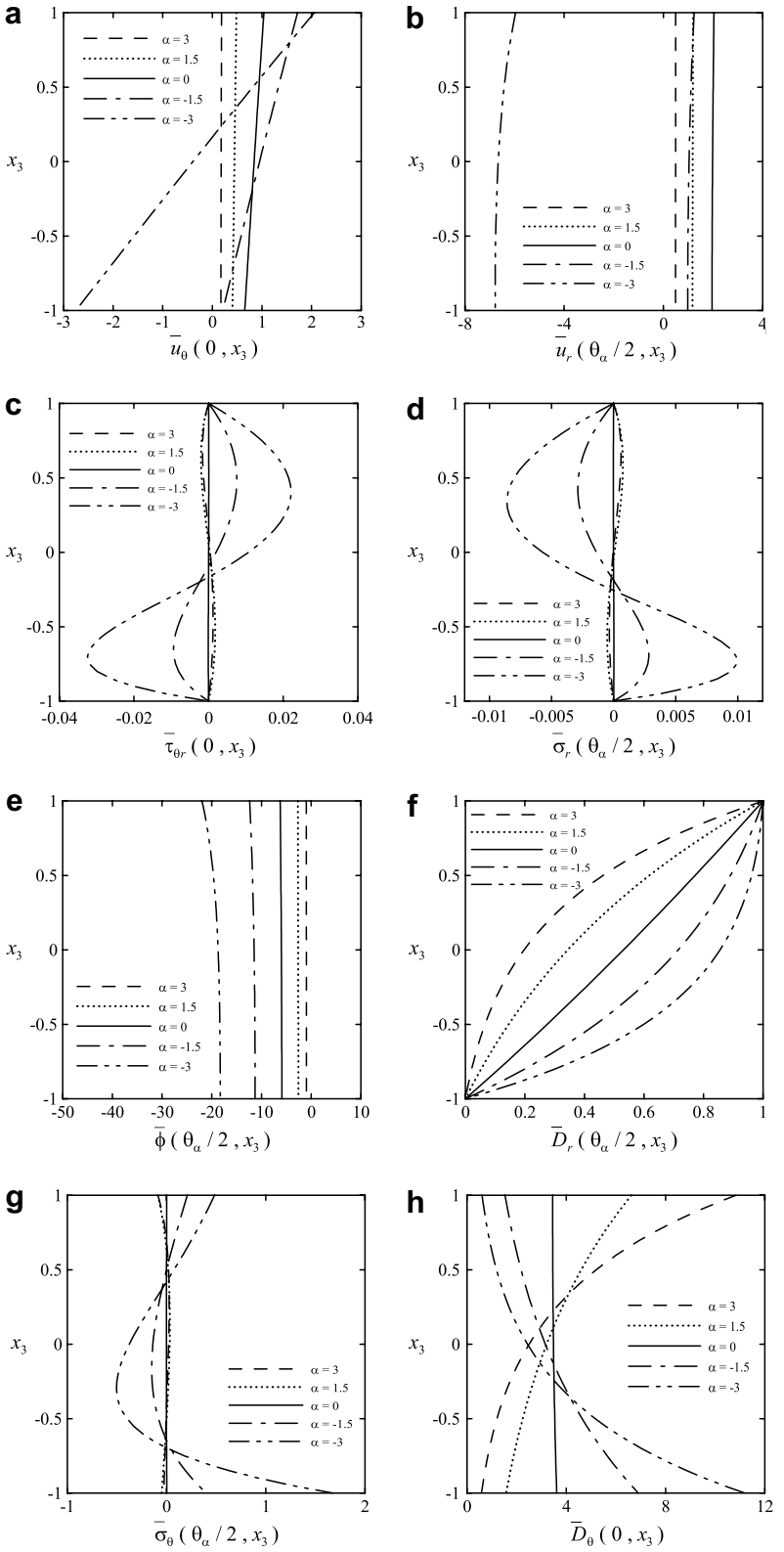

Fig. 6. Distributions of elastic and electric field variables through the thickness of FG piezoelectric cylindrical shell under cylindrical bending (Case 4).

The relative field variables are normalized as follows:
For loading condition of Case 1 (Eq. (124)),

$$\overline{u}_i = u_i c^*/q_0(2h), \quad \overline{\tau}_{ij} = \tau_{ij}/q_0, \quad \overline{\Phi} = \Phi e^*/q_0(2h), \quad \overline{D}_i = D_i c^*/q_0 e^*; \tag{134}$$

For loading conditions of Case 2 (Eq. (125)),

$$\overline{u}_i = u_i c^*/\phi_0 e^*, \quad \overline{\tau}_{ij} = \tau_{ij}(2h)/\phi_0 e^*, \quad \overline{\Phi} = \Phi/\phi_0, \quad \overline{D}_i = D_i c^*(2h)/\phi_0 (e^*)^2; \tag{135}$$

For loading conditions of case 4 (Eq. (127)),

$$\overline{u}_i = u_i e^*/D_0(2h), \quad \overline{\tau}_{ij} = \tau_{ij} e^*/D_0 c^*, \quad \overline{\Phi} = \Phi(e^*)^2/D_0 c^*(2h), \quad \overline{D}_i = D_i/D_0. \tag{136}$$

where $c^* = 10 \times 10^9$ N/m^2, $e^* = 10$ C/m^2, $q_0 = -1$ N/m^2, $\phi_0 = 1$ V, $D_0 = 1$ C/m^2.

The influence of material property gradient index on the mechanical and electric variables is studied among loading conditions of Cases 1, 2 and 4 in Figs. 4–6, respectively. Figs. 5(c) and (d) and 6(c) and (d) show that the through-the-thickness distributions of transverse stresses change dramatically as the index α becomes a positive value for Case 2; conversely, they change dramatically as the index α becomes a negative value for Case 4. The distributions of transverse stresses across the thickness coordinate in the Cases of 2 and 4 are higher-degree polynomials and are back and forth among the positive and negative values. It is also shown from Figs. 4(e) and (f) that the distributions of normal electric displacement through the thickness coordinate are approximately linear functions and parabolic functions for electric potential in Case 1. The through-the-thickness distributions of electric potential and normal electric displacement in Figs. 5(e) and (f) and 6(e) and (f) are shown to be different patterns between homogeneous piezoelectric shells ($\alpha = 0$) and FG piezoelectric shells in the cases of applied electric loads. By observation through Figs. 4–6, we found that the distributions of mechanical and electric variables through the thickness coordinate in FG piezoelectric shells reveal different patterns from homogeneous piezoelectric shells. Hence, it is suggested that an advanced 2D theory may be necessary to be developed for the analysis of FG piezoelectric shells, especially when the shells are subjected to electric loads.

8. Concluding remarks

Based on the method of perturbation, we develop two asymptotic formulations for the coupled static analysis of FG piezoelectric shells under two cylindrical bending types of electric loads. After a dimensional analysis, we select two different sets of dimensionless variables of electric field in conjunction with one identical set of those of elastic field. Through the complicated but straightforward manipulation, such as nondimensionalization, asymptotic expansions, successive integration etc, we obtain two recursive sets of governing equations for various order problems. In the cases of prescribed normal electric displacement, the variable of electric potential becomes as one of the generalized kinematics field variables in the governing equations for various order problems; whereas the variable of normal electric displacement becomes so in the cases of prescribed electric potential. These formulations are illustrated to be feasible in a systematic manner. Applications of the present formulations to illustrated examples show that the present solutions are accurate and the rate of convergence is rapid. It is noted that the through-the-thickness distributions of field variables in FG piezoelectric shells reveal different patterns from those in homogenous piezoelectric shells. According to the present analysis, we suggest that an advanced 2D theory may be necessary to be developed for the analysis of multilayered and FG piezoelectric shells, especially when the shells are subjected to electric loads.

Acknowledgement

This work is supported by the National Science Council of Republic of China through Grant NSC 95-2211-E006-464.

References

Chen, C., Shen, Y., Liang, X., 1999. Three dimensional analysis of piezoelectric circular cylindrical shell of finite length. Acta Mechanica 134, 235–249.

Chen, C.Q., Shen, Y.P., Wang, X.M., 1996. Exact solution of orthotropic cylindrical shell with piezoelectric layers under cylindrical bending. International Journal of Solids and Structures 33, 4481–4494.

Dumir, P.C., Dube, G.P., Kapuria, S., 1997. Exact piezoelectric solution of simply-supported orthotropic circular cylindrical panel in cylindrical bending. International Journal of Solids and Structures 34, 685–702.

Heyliger, P., 1997. A note on the static behavior of simply-supported laminated piezoelectric cylinders. International Journal of Solids and Structures 34, 3781–3794.

Heyliger, P., Brooks, S., 1996. Exact solutions for laminated piezoelectric plates in cylindrical bending. Journal of Applied Mechanics 63, 903–910.

Heyliger, P., Ramirez, G., 2000. Free vibration of laminated circular piezoelectric plates and discs. Journal of Sound and Vibration 229, 935–956.

Kapuria, S., Sengupta, S., Dumir, P.C., 1997. Three-dimensional solution for a hybrid cylindrical shell under axisymmetric thermoelectric load. Archive of Applied Mechanics 67, 320–330.

Lu, P., Lee, H.P., Lu, C., 2006. Exact solutions for simply supported functionally graded piezoelectric laminates by Stroh-like formalism. Composite Structures 72, 352–363.

Pan, E., 2001. Exact solution for simply supported and multilayered magneto-electro-elastic plates. Journal of Applied Mechanics 68, 608–618.

Pan, E., Han, F., 2005. Exact solution for functionally graded and layered magneto-electro-elastic plates. International Journal of Engineering Science 43, 321–339.

Ramirez, F., Heyliger, P.R., Pan, E., 2006a. Static analysis of functionally graded elastic anisotropic plates using a discrete layer approach. Composiste: Part B 37, 10–20.

Ramirez, F., Heyliger, P.R., Pan, E., 2006b. Free vibration response of two-dimensional magneto-electro-elastic laminated plates. Journal of Sound and Vibration 292, 626–644.

Ray, M.C., Rao, K.M., Samanta, B., 1992. Exact analysis of coupled electroelastic behavior of a piezoelectric plane under cylindrical bending. Computers & Structures 45, 667–677.

Tiersten, H.F., 1969. Linear Piezoelectric Plate Vibrations. Plenum Press, New York.

Vel, S.S., Mewer, R.C., Batra, R.C., 2004. Analytical solutions for the cylindrical bending vibration of piezoelectric composite plates. International Journal of Solids and Structures 41, 1625–1643.

Wang, X., Zhong, Z., 2003. Three-dimensional solution of smart laminated anisotropic circular cylindrical shells with imperfect bonding. International Journal of Solids and Structures 40, 5901–5921.

Wu, C.P., Chi, Y.W., 2005. Three-dimensional nonlinear analysis of laminated cylindrical shells under cylindrical bending. European Journal of Mechanics A/Solids 24, 837–856.

Wu, C.P., Chiu, S.J., 2002. Thermally induced dynamic instability of laminated composite conical shells. International Journal of Solids and Structures 39, 3001–3021.

Wu, C.P., Lo, J.Y., Chao, J.K., 2005. A three-dimensional asymptotic theory of laminated piezoelectric shells. CMC-Computers, Materials, & Continua 2, 119–137.

Wu, C.P., Lo, J.Y., 2006. An asymptotic theory for the dynamic response of laminated piezoelectric shells. Acta Mechanica 183, 177–208.

Wu, C.P., Tarn, J.Q., Chi, S.M., 1996. An asymptotic theory for dynamic response of doubly curved laminated shells. International Journal of Solids and Structures 33, 3813–3841.

Zhong, Z., Shang, E.T., 2003. Three-dimensional exact analysis of a simply supported functionally gradient piezoelectric plate. International Journal of Solids and Structures 40, 5335–5352.

Zhong, Z., Shang, E.T., 2005. Exact analysis of simply supported functionally graded piezo-thermoelectric plates. Journal of Intelligent Material Systems and Structures 16, 643–651.